Cell. Mol. Life Sci. (2012) 69:981–992
DOI 10.1007/s00018-011-0818-z

Cellular and Molecular Life Sciences

RESEARCH ARTICLE

Tissue transglutaminase inhibits the TRPV5-dependent calcium transport in an N-glycosylation-dependent manner

Sandor Boros · Qi Xi · Henrik Dimke · Annemiete W. van der Kemp · Kukiat Tudpor · Sjoerd Verkaart · Kyu Pil Lee · René J. Bindels · Joost G. Hoenderop

Received: 6 April 2011 / Revised: 25 August 2011 / Accepted: 6 September 2011 / Published online: 28 September 2011

Abstract Tissue transglutaminase (tTG) is a multifunctional Ca^{2+}-dependent enzyme, catalyzing protein crosslinking. The transient receptor potential vanilloid (TRPV) family of cation channels was recently shown to contribute to the regulation of TG activities in keratinocytes and hence skin barrier formation. In kidney, where active transcellular Ca^{2+} transport via TRPV5 predominates, the potential effect of tTG remains unknown. A multitude of factors regulate TRPV5, many secreted into the pro-urine and acting from the extracellular side. We detected tTG in mouse urine and in the apical medium of polarized cultures of rabbit connecting tubule and cortical collecting duct (CNT/CCD) cells. Extracellular application of tTG significantly reduced TRPV5 activity in human embryonic kidney cells transiently expressing the channel. Similarly, a strong inhibition of transepithelial Ca^{2+} transport was observed after apical application of purified tTG to polarized rabbit CNT/CCD cells. Furthermore, tTG promoted the aggregation of the plasma membrane-associated fraction of TRPV5. Using patch clamp analysis, we observed a reduction in the pore diameter after tTG treatment, suggesting distinct structural changes in TRPV5 upon crosslinking by tTG. As N-linked glycosylation of TRPV5 is a key step in regulating channel function, we determined the effect of tTG in the N-glycosylation-deficient TRPV5 mutant. In the absence of N-linked glycosylation, TRPV5 was insensitive to tTG. Taken together, these observations imply that tTG is a novel extracellular enzyme inhibiting the activity of TRPV5. The inhibition of TRPV5 occurs in an N-glycosylation-dependent manner, signifying a common final pathway by which distinct extracellular factors regulate channel activity.

Keywords TRPV5 · Calcium channel · Transepithelial Ca^{2+} transport · Transglutaminase

Abbreviations

Ca^{2+}	Calcium ion
CNT/CCD	Connecting tubule/cortical collecting duct
DMA^+	Dimethylammonium
HA tag	Hemagglutinin tag
HEK293 cells	Human embryonic kidney 293 cells
I_X	Ionic current
I/*V* relationship	Current–voltage relationship
MA^+	Monomethylammonium,
Na^+	Sodium ion
$NMDG^+$	*N*-methyl-D-glucamine chloride
PMSF	Phenylmethylsulfonyl fluoride
P_X/P_{Na}	Relative permeability
$TetMA^+$	Tetramethylammonium
$TriMA^+$	Trimethylammonium
TRPV5	Transient receptor potential vanilloid type 5
tTG	Tissue transglutaminase

Introduction

Maintenance of the systemic Ca^{2+} concentration is essential for many physiological processes, ranging from enzyme activation to bone mineralization. As such, the kidney plays a key role in stabilizing plasma Ca^{2+} by

S. Boros · Q. Xi · H. Dimke · A. W. van der Kemp · K. Tudpor · S. Verkaart · K. P. Lee · R. J. Bindels · J. G. Hoenderop (✉)
286 Department of Physiology,
Radboud University Nijmegen Medical Centre,
P.O. Box 9101, 6500 HB Nijmegen, The Netherlands
e-mail: J.Hoenderop@fysiol.umcn.nl

changing the urinary excretion of Ca^{2+} in response to excess or depletion of this divalent cation [15, 39, 40]. In kidney, Ca^{2+} is reabsorbed primarily via a passive paracellular pathway along the proximal tubule and the thick ascending loop of Henle [40]. Approximately 10% of the Ca^{2+} load re-enters the bloodstream via an active transcellular transport process in the distal part of the nephron [16, 40]. The transient receptor potential vanilloid type 5 (TRPV5) cation channel facilitates the apical uptake of Ca^{2+} in these segments [17]. In rabbit, TRPV5 is expressed predominantly in the collecting tubule (CNT), while in other species, such as mouse and rat, substantial expression of the channel is also observed in the distal convoluted tubule (DCT) [16, 26]. Ablation of TRPV5 in mice ($TRPV5^{-/-}$) impairs transcellular Ca^{2+} reabsorption, resulting in robust hypercalciuria and compensatory vitamin D-dependent hyperabsorption [18].

TRPV5 has unique electrophysiological characteristics, including the constitutive inward rectifying activity at low intracellular Ca^{2+} concentrations and physiological membrane potentials, Ca^{2+}-dependent inactivation and selectivity for Ca^{2+} [29]. Monomers of TRPV5 associate into functional tetramers by facing each other with their pore-forming regions [19]. Furthermore, a single conserved N-glycosylation site at asparagine-358 (N358), harbored in the first extracellular loop is another important structural feature of TRPV5. Native TRPV5 has been shown to undergo N-glycosylation, resulting in high mannose and complex-glycosylated proteins [19]. The activity of TRPV5 is controlled at multiple levels by an array of different factors, including calciotropic hormones (e.g., 1,25-dihydroxyvitamin D3) and extracellular factors (e.g., the glycosidase klotho) [9, 30, 41]. Klotho, as an extracellular glycosidase [8, 9], hydrolyzes oligosaccharide chains from the complex N-glycan of TRPV5. This extracellular modification results in delayed retrieval of the Ca^{2+} channel from the apical plasma membrane and subsequently increases Ca^{2+} transport [8, 9]. The stimulatory effect of klotho is entirely dependent on the N-glycosylation of TRPV5, suggesting that the N-glycosylation status of TRPV5 is crucial for this type of extracellular regulation [8, 9].

Tissue transglutaminase (tTG, also known as TGase2; EC 2.3.2.13) is a multifunctional protein catalyzing the Ca^{2+}-dependent covalent crosslinking of specific lysine (Lys) and glutamine (Gln) residues of substrate proteins [13, 27]. Interestingly, several Ca^{2+}-binding proteins are known substrates of tTG. Calbindin-D_{28K}, an intracellular protein involved in Ca^{2+}-binding playing a key role in transcellular Ca^{2+} transport, has been shown to be a substrate of tTG [11, 44]. Furthermore, several members of the family of S100A EF-hand proteins are also substrates of tTG [6, 34]. This includes S100A10, which is involved in the forward trafficking of TRPV5 to the plasma membrane [34, 42].

A recent study by Cheng et al. elegantly showed that TRPV3, another member of the TRPV family, contributes in part to epidermal barrier function by affecting the activity of transglutaminase [10]. This is likely to occur via increased TRPV3-dependent Ca^{2+} influx and subsequent Ca^{2+}-dependent activation of the enzyme. In addition to these observations, TGase1 expression has also been shown to be regulated by TRPV6 during Ca^{2+}-induced differentiation of keratinocytes [24]. Transporters in the renal epithelium can be directly affected by extracellular factors found in the urine, secreted by the cells themselves or filtered by the glomerulus from the blood, constituting a unique environment. tTG is found in the intracellular compartment, but the enzyme is also secreted, indicating that, in these epithelia, the enzyme could act from the urinary side. In terms of TRPV5-dependent transport, such a mechanism could suggest an alternative mode of regulation, in comparison to what is observed in, e.g., the skin barrier formation. Our experiments describe the identification of tTG as a novel molecular inhibitor of TRPV5. We find that the kidney secretes tTG into the pro-urine where it covalently crosslinks TRPV5 from the extracellular compartment and thereby changes the pore size of the channel in an N-glycosylation-dependent manner.

Materials and methods

DNA constructs

The pCINeo/IRES-GFP plasmid encoding HA-TRPV5 was generated as described previously [42]. HA-TRPV5-N358Q was obtained by in vitro mutagenesis of HA-TRPV5-pCINeo/IRES-GFP cDNA according to the manufacturer's instructions (Stratagene, La Jolla, CA, USA) [9]. All constructs were verified by DNA sequence analysis.

Cell lines and transfections

Human embryonic kidney (HEK293) cells were cultured in Dulbecco's modified essential medium (DMEM) supplemented with 10% v/v fetal calf serum and 2 mM L-glutamine. For cell surface biotinylation experiments, cells were transiently transfected in Petri-dishes, using polyethyleneimine (PEI).

Collection and concentration of pre-conditioned culture medium

CNT/CCD cells were isolated from New Zealand White rabbits as described previously [4], and grown to confluence on 0.33-cm^2 permeable filter supports (Corning-Costar, Cambridge, MA, USA). Apical and basolateral

media were collected after seeding the cells on permeable supports. All collected media were concentrated three times (Millipore), and salts and proteins <30 kDa were removed by using centriprep ultracel-YM-30 columns (Millipore, Bedford, MA, USA) as described [9].

Immunoblotting, and protein concentration determination

TRPV5 and tTG protein expression was determined by SDS–PAGE followed by immunoblotting, using anti-HA (Cell Signaling, Danvers, USA), anti-tTG (Transglutaminase II Ab-4; Lab Vision/Immunologic, Duiven, The Netherlands, unless stated otherwise) and peroxidase-labeled rabbit anti-mouse IgG (Sigma-Aldrich, St. Louis, MO, USA) antibodies. Protein concentration was measured by using the bicinchoninic acid protein assay kit (Thermo Scientific, Rockford, IL, USA), according to the manufacturer's manual.

Cell surface biotinylation

HEK293 cells were transfected with HA-TRPV5 or HA-TRPV5-N358Q in pCINeo/IRES-GFP. One day after transfection, cells were re-seeded on poly-L-lysine-coated (0.1 mg/ml) culture dishes and incubated with guinea pig tTG (1 μg/ml; Sigma-Aldrich) for 6 h at 37°C, respectively. Subsequently, cells were biotinylated, and TRPV5 was precipitated from the cell lysates with neutravidin beads (Pierce, Etten-Leur, The Netherlands) as described previously [9]. Briefly, cells were collected from the plates and disrupted in 1 ml lysis buffer [1% v/v Triton X-100, 150 mM NaCl, 5 mM EDTA, 50 mM Tris (pH 7.5 adjusted with HCl), 1 mM PMSF, 5 μg/ml leupeptin, 5 μg/ml aprotinin, 1 μg/ml pepstatin-A], immediately after biotinylation. Cells were subsequently washed with ice-cold PBS, and homogenized in 1 ml lysis buffer, followed by precipitation using neutravidin beads. TRPV5 protein expression at the cell surface and in total cell lysates was measured as described above.

$^{45}Ca^{2+}$ uptake assay

HEK293 cells transfected with TRPV5 pCINeo/IRES-GFP constructs were cultured in 24-well plates and incubated with uptake buffer containing 110 mM NaCl, 5 mM KCl, 1.2 mM $MgCl_2$, 0.1 mM $CaCl_2$, 10 mM Na-acetate, 2 mM NaH_2PO_4, 20 mM HEPES–Tris, pH 7.4 supplemented with 10 μM felodipine, 10 μM methoxy-verapamil, and 1 μCi/ml $^{45}CaCl_2$ for 10 min at 37°C. After extensive washing with stop buffer (110 mM NaCl, 5 mM KCl, 1.2 mM $MgCl_2$, 0.5 mM $CaCl_2$, 1.5 mM $LaCl_3$, 10 mM Na-acetate, 20 mM HEPES–Tris, pH 7.4) at 4°C, cells were disrupted with 0.05% w/v SDS and radioactivity was counted using liquid scintillation.

Primary CNT and CCD cell cultures

Culture and infection of rabbit kidney connecting tubule and cortical collecting duct cells was as follows. Rabbit kidney CNT/CCD cells were immunodissected from the kidney cortex of New Zealand White rabbits (~0.5 kg) using antibody R2G9 and then placed in primary culture on permeable filters (0.33 cm^2; Costar, Cambridge, MA, USA) as described previously [4]. The culture medium was a 1:1 mixture of Dulbecco's modified Eagle's medium and Ham's F12 medium (DME/F12; Gibco, Paisley, UK) supplemented with 5% (v/v) decomplemented fetal calf serum, 50 μg/ml gentamicin, 10 μl/ml nonessential amino acids (Gibco), 5 μg/ml insulin, 5 μg/ml transferrin, 50 nM hydrocortisone, 70 ng/ml prostaglandin E1, 50 nM Na_2SeO_3, and 5 pM triiodothyronine, and equilibrated with 5% (v/v) CO_2 at 37°C. Transepithelial potential difference and resistance were routinely checked before and after every transport measurement to confirm cell confluency and integrity of the monolayer. Calcium transport measurements were performed as described [4].

Electrophysiology

Whole-cell currents were measured with an EPC-10 (HEKA Electronic, Lambrecht, Germany) amplifier using Patch master V2.20 software. The borosilicate glass electrode resistance was between 2.5 and 4 MΩ. The ramp protocol for measuring the current–voltage (*I*/*V*) relationship of Na^+ consisted of linear voltage ramps from −100 to +100 mV within 450 ms repeated every 5 s. The step protocol for measuring the Ca^{2+} current consisted of a 10-s-long voltage step applied from +70 to −100 mV. Current traces were sampled at 0.5 ms for the ramp and 2 ms for the step protocol. Current densities were calculated from the current at −80 mV during the ramp protocol. The standard extracellular solution contained 150 mM NaCl, 6 mM CsCl, 10 mM HEPES, 50 μM EDTA and 10 mM glucose (pH 7.4 adjusted with NaOH) for divalent free Na^+, and 10 mM $CaCl_2$ was supplemented for the Ca^{2+} measurement. The internal (pipette) solution contained 20 mM CsCl, 100 mM Cs-aspartate, 1 mM $MgCl_2$, 10 mM BAPTA, 4 mM NaCl, 2 mM ATP and 10 mM HEPES (pH 7.2 adjusted with CsOH). Data was analyzed using Igor-pro software (WaveMetrics, Oswego, OR, USA).

Pore measurements

The standard pipette solution contained Tris–HCl buffered 150 mM NaCl, 10 mM EDTA and 10 mM HEPES (pH 7.2 adjusted with Tris–HCl) whereas the extracellular solution contained 150 mM NaCl and 10 mM HEPES (pH 7.4 adjusted with Tris–HCl). The relative permeabilities (P_X^+/P_{Na}^+) of mono-, di-, tri- and tetramethylammonium derivatives and of *N*-methyl-D-glucamine chloride ($NMDG^+$) were measured using solutions in which Na^+ was substituted by the respective cations. Reversal potentials were calculated from the bi-ionic reversal potentials; furthermore, all potentials were corrected for possible liquid junction potentials calculated according to Barry et al. [2]. In these permeation experiments, the standard pipette solution was used as intracellular solution. For the ammonium derivates, the following compound diameters were used (in nm): 0.36, 0.46, 0.52, 0.58 and 0.68 for monomethylammonium (MA^+) dimethylammonium (DMA^+), trimethylammonium ($TriMA^+$), tetramethylammonium ($TetMA^+$) and for $NMDG^+$ (all compounds obtained from Sigma), respectively. For curve-fitting, the points from the graph plotting permeability ratios of the different organic cations (X) versus the estimated diameters, the excluded volume considering friction of the permeating ion Eq. $P_X^+/P_{Na}^+ = k(1 - a/d)^2/a$ was used [2], where a is the organic cation diameter, k the constant factor and d is the minimal pore diameter.

Statistical analysis

In all experiments, the data were expressed as mean ± SEM. Statistical significance ($P < 0.05$) was determined by analysis of variance (ANOVA) and a Bonferroni post-hoc test.

Results

tTG is secreted into the pro-urine and into the apical medium of CNT/CCD cells

Twenty-four-hour urine samples from wild-type mice were desalted, concentrated and the total amounts were subsequently analyzed for tTG expression by SDS–PAGE followed by tTG Western blotting. A band with a molecular size slightly above 75 kDa was observed in urine samples (Fig. 1a), corresponding to the known 75–78 kDa size of tTG. Since tTG was detected in the 24-h urine of mice, we next analyzed the expression levels of tTG in the CNT/CCD region. To this end, polarized primary cultures of rabbit CNT/CCD were used. Western blot analysis, wherein β-actin was used as loading control, revealed that polarized CNT/CCD cells abundantly express tTG (Fig. 1b, upper panel). In the apical conditioned media of primary CNT/CCD cells a significant amount of tTG could be detected (Fig. 1c, upper panel). In addition, tTG was also abundantly present in the basolateral compartment (Fig. 1c, lower panel.

tTG inhibits the activity of TRPV5

First, we investigated the dose response relationship between tTG and TRPV5 by radioactive Ca^{2+} uptake measurements. To this end, we used a commercial tTG purified from guinea pig liver. The enzyme had a minimum of 80% purity demonstrated by SDS–PAGE and in line with specifications of the vendor Sigma (data not shown). TRPV5 expressing HEK293 cells were irresponsive to low concentration tTG (10^{-4} to 10^{-2} µg/ml), but a strong reduction in the Ca^{2+} influx was observed in the presence of 0.1–30 µg/ml tTG, with an EC_{50} of 5 µg/ml (Fig. 2a). Next, we analyzed whether the inhibitory effect of tTG on TRPV5-mediated Ca^{2+} uptake could be reversed by co-incubation of tTG in the presence of the tTG inhibitors cadaverine or cystamine. To this end, HEK293 cells transiently expressing TRPV5 were treated with tTG (1 µg/ml) for 6 h in the absence or presence of cadaverine or cystamine. As depicted in Fig. 2b, both cadaverine and cystamine can reverse the inhibitory effect of tTG on TRPV5. Heat-inactivated tTG (95°C heat denaturation for 10 min) was not able to inhibit TRPV5-mediated Ca^{2+} uptake.

In addition, we investigated whether tTG can directly affect the activity of the TRPV5 channel. HEK293 cells transiently expressing the channel were treated with tTG (1 µg/ml), for 6 h and subjected to patch clamp analysis (Fig. 2c). Heterologous overexpression of TRPV5 yielded a large, approximately 1,500-pA/pF Na^+ current density (Fig. 2c). Incubation with tTG for 6 h resulted in a significant, 50% reduction of the current density (Fig. 2c). Additionally, the tTG inhibitor cadaverine (150 µM) prevented the tTG-mediated inhibition of TRPV5 (Fig. 2c, d). Normalizing the Na^+ currents (I_{Na}^+/I_{Na}^+max) showed that only the tTG-treated TRPV5 changed its conducting properties (Fig. 2d, inset). Furthermore, compared with control, we could also observe a significantly reduced TRPV5 Ca^{2+} current upon tTG administration (Fig. 2e).

The inhibitory effect of tTG was further investigated by transcellular Ca^{2+} transport assays in polarized rabbit primary CNT/CCD cell monolayers. The forskolin-stimulated transcellular Ca^{2+} transport was significantly reduced by tTG added on the apical, but not on the basolateral side, and this inhibitory effect of the enzyme could be prevented

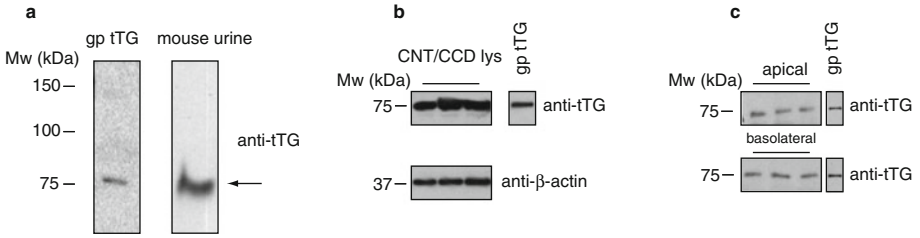

Fig. 1 tTG is secreted into mouse urine and into the apical media of rabbit primary CNT/CCD cells. **a** Mice ($n = 3$) were housed in metabolic cages and 24-h urine samples were collected. Samples were concentrated and subsequently analyzed for tTG expression by SDS–PAGE followed by anti tTG Western blotting. **b** Isolated rabbit primary CNT/CCD cells were allowed to polarize on filter supports. Polarized monolayers ($n = 3$) were probed for tTG expression by SDS–PAGE and subsequent immunoblot with anti-tTG (*upper panels*), and anti-β-actin antibodies (*lower panels*), respectively. **c** Apical and basolateral media from polarized CNT/CCD cells were collected and concentrated, and subsequently analyzed for tTG secretion by immunoblotting

by the tTG blocker cadaverine (Fig. 2f). Although endogenous tTG could be detected in the primary cultures, incubating the cells with cadaverine did not result in a detectable change in transcellular Ca^{2+} transport (Fig. 2f).

To address whether tTG reduces the number of channels at the plasma membrane, the action of tTG on TRPV5 was assessed by cell surface biotinylation studies. TRPV5, with molecular masses between approximately 70 and 85 kDa, representing the core and complex glycosylated monomers of the channel, respectively, were detected in the plasma membrane fraction (Fig. 2g). Compared to the control (-tTG), a decrease in the amount of TRPV5 monomers was observed after tTG treatment (Fig. 2f). More importantly, after incubation with tTG, TRPV5 oligomers with a molecular mass of $\sim$250 kDa were observed (Fig. 2g).

tTG reduces the pore diameter of TRPV5

To estimate whether tTG-induced aggregation of TRPV5 can affect the pore of the channel, the pore diameter was determined both in the absence and the presence of the enzyme. First, the Na^+ and Ca^{2+} currents were recorded in the absence and presence of tTG, revealing a significant reduction in both the Na^+ and the Ca^{2+} currents upon tTG administration (Fig. 3a, b). Next, the permeability ratios of currents carried by organic monovalent cations of increasing size relative to Na^+ current were measured. When Na^+ was used as the sole charge carrier, the current reverted close to 0 mV with a clearly inward-rectifying shape (Fig. 3c, gray curve). Next, all Na^+ ions from the extracellular solution were substituted by monomethylammonium or its di-, tri- and tetramethyl derivatives (MA^+, DMA^+, $TriMA^+$, $TetMA^+$) and finally by the larger organic cation *N*-methyl-D-glucamine ($NMDG^+$). To a lesser extent, these cations, were also able to permeate TRPV5, and the recorded currents were directly proportional to the size of each cation (Fig. 3d–h, gray curves). Incubation with tTG resulted in significantly smaller currents in the case of all cations except $NMDG^+$, which showed virtually no change compared to control (Fig. 3d–h, black curves). Furthermore, a negative shift in the reversal potential of MA^+, DMA^+, $TriMA^+$ was observed (Fig. 3d, f, insets).

The permeability ratios, relative to Na^+ (P_X^+/P_{Na}^+), were calculated from the recorded bi-ionic reversal potentials for all five cations (MA^+, DMA^+, $TriMA^+$, $TetMA^+$ and $NMDG^+$) for untreated and tTG-treated HEK293 cells expressing TRPV5, and subsequently plotted against the estimated diameter of each cation. Compared to control tTG clearly reduced the P_X^+/P_{Na}^+ ratios of TRPV5 in the cases of MA^+, DMA^+, $TriMA^+$ (Fig. 3i, dashed line). Next, using the permeability ratios, the pore diameters were calculated. In the control situation, the pore diameter for TRPV5 was calculated to be 6.44 $\pm$ 0.01 Å (Fig. 3j). Treatment with tTG resulted in a slight but significant decrease in the pore size as the diameter was calculated to be 5.79 $\pm$ 0.02 Å (Fig. 3j).

N-glycosylation of TRPV5 is important for tTG-mediated inhibition

The N-glycan of TRPV5 is crucial for its regulation by extracellular factors, such as klotho. We next tested this was also the case for the inhibitory effect of tTG. To this end, HEK293 cells expressing the N-glycosylation-deficient mutant form of the channel (HA-TRPV5-N358Q) were treated with tTG and subjected to patch clamp and cell surface biotinylation analyses. Patch clamp recordings showed similar Na^+ currents for the untreated wild-type and the mutant form of TRPV5 (Fig. 4a). However, tTG incubation reduced the activity of the wild-type channel, but not of TRPV5-N358Q (Fig. 4a, b). This was further substantiated by normalizing the Na^+ currents (Fig. 4c) as changes in the curve shape could be observed only for the

tTG-treated wild-type TRPV5 current. Cell surface labeling of HEK293 cells expressing either the wild-type TRPV5-N358Q showed abundant expression of both wild-type and mutant TRPV5 at the plasma membrane (Fig. 4d, upper panel). Treatment with tTG caused the aggregation of TRPV5 at the plasma membrane and concomitantly decreased the amount of wild-type TRPV5 monomers (Fig. 4d, upper panel, and e). However, this aggregation could not be observed in the case of the mutant channel (Fig. 4d, upper panel, and e). Additionally, incubation with tTG did not alter the total expression of the wild-type or the mutant form of TRPV5 (Fig. 4d). Semi-quantitative analysis of the signal intensities further substantiated the previous findings as the percentage of aggregation was found to be significant only in the case of the tTG-treated wild-type TRPV5 (Fig. 4e).

Finally, we investigated the binding capacity of tTG to wild-type and the N-glycosylation deficient TRPV5 channels. The immunoprecipitated wild-type and mutant TRPV5 were incubated with or without tTG at 4°C in the absence of Ca^{2+} to reduce the enzymatic activity of tTG. These immunoprecipitation experiments revealed that tTG binds to both wild-type and the mutant form of TRPV5 with equal affinity (Fig. 4f).

Fig. 2 tTG inhibits TRPV5-mediated currents and transcellular Ca^{2+} ▶ transport in primary CNT/CCD cells. **a** Dose response relationship between tTG and TRPV5. HEK293 cells expressing TRPV5 were treated with different concentrations of tTG 10^{-4} to 3×10^{1} μg/ml and subjected to $^{45}Ca^{2+}$ uptake. **b** tTG inhibited $^{45}Ca^{2+}$ uptake via TRPV5 is counteracted by the tTG inhibitors cystamine and cadaverine. HEK293 cells transfected with TRPV5 pCINeo/IRES-GFP or pCINeo/IRES-GFP (mock) constructs were treated with active or inactive tTG (1 μg/ml for 6 h), in the presence or absence of cadaverine (150 μM) and cystamine (50 mM). After treatment, the effect of tTG was assayed in radiotracer experiments following the protocol described in "Materials and methods". **c** tTG directly inhibits the activity of TRPV5. Na^+ *I/V* relations were measured from TRPV5-transfected HEK293 cells. The cells were subjected to 6-h tTG treatment (1 μg/ml) in the presence and absence of cadaverine (150 μM) before the current measurements. Data are shown as mean ± SEM. *Asterisk* indicates significant difference from the cells expressing TRPV5 ($n = 15$; $P < 0.05$). **d** Representative Na^+ *I/V* relations of TRPV5 treated with tTG in the absence or presence of cadaverine. *Inset* Na^+ currents from panel **c** were normalized to I_{Na} max for better comparison. **e** Representative Ca^{2+} currents of untreated and tTG-treated TRPV5. **f** Polarized rabbit primary CNT/CCD cells were treated for 6 h with 1 μg/ml apically and basolaterally administered tTG and transport was measured as described previously [23]. Data are shown as mean ± SEM. *Asterisk* indicates significant difference from the control situation ($n = 15$; $P < 0.05$). **g** Cell surface biotinylation of HEK293 cells transiently transfected with pCINeo-HA-TRPV5/IRES-GFP and treated for 6 h with 1 μg/ml tTG. After treatment, cells were subjected to cell surface biotinylation, followed by neutravidin pull-down. The *upper* and the *lower panels* represent the biotinylated cell surface fractions and the total cell lysates, respectively. Lysates were separated on SDS–PAGE and blots were probed with an anti-HA antibody

Discussion

Active transcellular Ca^{2+} transport in the kidney takes place exclusively in the DCT/CNT segments of the nephron, where the epithelial Ca^{2+} channel TRPV5 controls the Ca^{2+} entry. In this study, we identified tTG as a novel inhibitor of TRPV5 activity, acting from the extracellular side in a N-glycosylation-dependent manner. This conclusion is based on the following observations: (1) tTG is found in the urine in mice, in line with the expression and secretion of the enzyme in polarized primary CNT/CCD cells; (2) tTG decreases the activity of TRPV5 in transiently transfected HEK293 cells and inhibits transcellular Ca^{2+} transport in polarized primary CNT/CCD cells; (3) crosslinking of TRPV5 by tTG results in a decrease in the pore size of the channel; and (4) the inhibitory effect of tTG depends on the N-glycosylation state of TRPV5 as the N-glycosylation-deficient mutant is not susceptible to tTG-catalyzed modifications.

Increased expression and activity of tTG have been previously observed in renal disorders such as diabetic nephropathy or chronic kidney disease [12, 20, 21, 25, 36, 38]. In these diseases, tTG activity has been associated with tissue fibrosis and scar formation, taking place in the extracellular matrix [12, 37]. However, whether tTG is secreted into the urine during these conditions has not been tested. We established the presence of tTG in the urine of mice, which together with the fact that primary cultures of polarized rabbit CNT/CCD cells also secrete a fraction of endogenously expressed tTG into the apical medium suggests that tTG is present in the pro-urine. Though tTG is secreted into the apical medium of primary CNT/CCD cultures, transcellular Ca^{2+} transport was not affected by cadaverine in these cells. An insufficient concentration of endogenous tTG may explain such a discrepancy. In line with this, one may envisage that in renal disorders the amount of tTG in the urine is sufficient for an effective inhibition of TRPV5. The possibility that the endogenous tTG in these extracellular compartments is present in a catalytically inactive, so-called closed state is also feasible [31]. The presence of tTG has been reported previously in the DCT region and also in other nephron segments [12, 21, 37]. Tubular secretion is, therefore, likely to contribute to the amount of tTG found in the urine. These observations imply that tTG could function as a novel urinary factor, involved in regulating Ca^{2+} reabsorption in the distal part of the nephron.

Patch clamp recordings of TRPV5 and transcellular transport assays in primary CNT/CCD cells showed a

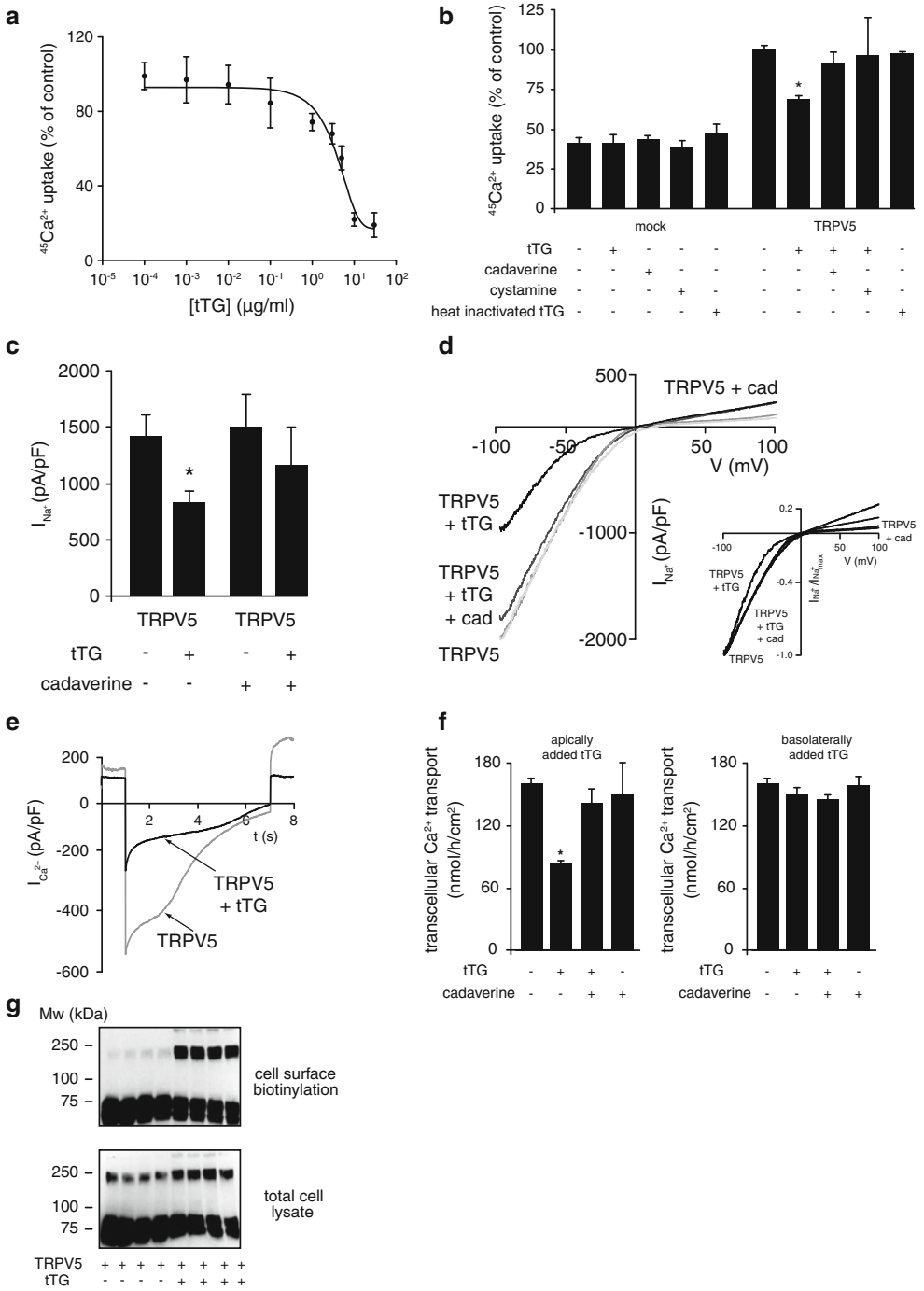

significant inhibitory effect of tTG on Ca^{2+} transport. Earlier studies have reported that tTG has the ability to modify the activity of the large conductance Ca^{2+}-activated K^+ (Maxi-K) channel [23]. Using the non-hydrolysable GTP analogue GTPγS, these studies showed that the GTPγS-stimulated channel activity is decreased to control levels when cells are treated with an antibody against tTG [23]. Such a G-protein-like effect of tTG on TRPV5 is unlikely, as cadaverine, the inhibitor of the crosslinking activity of the enzyme, abolishes the effect of tTG. Next to the functional assays, cell surface biotinylation studies revealed the formation of SDS-resistant, probably covalently crosslinked, TRPV5 aggregates in the plasma membrane upon tTG incubation. tTG is known to

be externalized into the extracellular space where it crosslinks and therefore stabilizes the heteromeric assemblies of several matrix and basolateral membrane proteins [1, 3, 22, 32, 33]. In the case of the tTG substrate small heat shock proteins (αB-crystallin, Hsp27, Hsp20 and HspB2), crosslinking between different small heat shock proteins has been demonstrated to be more efficient when they interact with each other in the same macromolecular assembly [5]. These observations suggested that tTG-substrate proteins in close proximity to each other are more prone to crosslinking than those existing in different complexes. TRPV5 exists in a homotetrameric form, as four monomers need to associate into operational tetramers prior to plasma membrane insertion [19]. Furthermore, it also harbors several glutamine and lysine residues facing the extracellular environment. Since the extracellular environment as well as the pro-urine contains sufficient amounts of Ca^{2+} for the activation of tTG, the tTG-mediated aggregation of TRPV5 monomers could take place from the extracellular side.

tTG did not change the protein stability, membrane expression or trafficking/recycling properties of TRPV5. Instead, we found that extracellular addition of tTG decreases the pore size of TRPV5. TRPV5 harbors several glutamines and two lysines in the first extracellular loop, which are the potential substrate sites for tTG. Crosslinking these sites could introduce extra rigidity or tension into the structure of the membrane-inserted TRPV5 in such a way that it could cause either a slight deformation in the dynamic structure of the pore and a subsequent reduction in ion permeability. Previously, acidification of both the intra- and extracellular environment has been shown to decrease the pore diameter of TRPV5 by intracellular pH [7]. tTG reduced the pore size by 10%, which is similar to the decrease observed upon acidification [7], suggesting that such a degree of reduction could already account for the decreased channel activity. We propose a tentative model how this change in the pore size could inhibit the activity of TRPV5. Crosslinking of TRPV5 may cause extra rigidity in the channel, which in turn results in a smaller pore size. This decrease could inhibit the influx of Ca^{2+} more efficiently than that of Na^+, as the flow of Na^+ is continuous in the pore, whereas Ca^{2+} migrates in the pore through a Ca^{2+}-binding pocket, which could be less accessible to Ca^{2+} due to the rigidity of the channel (Fig. 3k). Our observations suggest that not only pH changes, but also tTG, could inhibit the activity of TRPV5 by reducing its pore size.

N-glycosylation of TRPV5 is crucial for the extracellular regulation of the channel by klotho [8, 9]. Surprisingly, tTG had no inhibitory effect on TRPV5-N358Q, suggesting that the presence of the sugar tree is critical for tTG action. Negatively charged glycosaminoglycans such as heparin are known to bind tTG [14, 35, 43]. We speculated that the sialic acid-containing, and therefore negatively charged, N-glycan of TRPV5 may bind tTG, providing better accessibility to the substrate sites located in the vicinity of the N-glycan. However, co-immunoprecipitation experiments showed that tTG binds equally to both the wild-type and to the N-glycosylation-deficient TRPV5 mutant. Because of the equal binding efficiency, the substrate site exposure is more likely to depend on the N-glycosylation status of TRPV5. Klotho (as well as other glycosidases) can hydrolyze sugar residues from the N-glycan of TRPV5 and thereby increase the activity of the channel [8, 9, 28]. Modification of the N-glycan by klotho might safeguard TRPV5 from the tTG-mediated inhibition. However, further experiments should clarify the presence of such cross-talk between klotho and tTG. The fact that these different enzymes require intact N-glycosylation of TRPV5 for their actions could imply a central role for the N-glycan in the extracellular regulation of the channel.

Fig. 3 tTG decreases the pore diameter of TRPV5. **a** TRPV5 Na^+ current density in the absence and presence of tTG (for details see legends for Fig. 2). **b** TRPV5 Ca^{2+} current density in the absence and presence of tTG. The cells were subjected to 6-h tTG treatment (1 μg/ml). Data are shown as mean ± SEM. *Asterisk* indicates significant difference from the cells expressing TRPV5 ($n = 15$; $P < 0.05$). **c–h** Representative current voltage relationships of the different ions in the absence and presence of tTG. **c** shows the IV for Na^+, **d**, **e**, **f**, **g**, and **h** are the IV plots for MA^+, DMA^+, $TriMA^+$, $TetMA^+$ and $NMDG^+$, respectively ($n = 7$). The currents carried by organic monovalent cations were measured using solutions in which Na^+ was substituted by the respective cations. *Arrows* with *continuous* and *dashed lines* indicate the reversal potential in the untreated and the tTG-treated samples, respectively. The *insets* in **c–h** display the *I/V* relations in an expanded scale to show the reversal potentials. **i** Calculated relative permeability ratios of untreated and tTG-treated TRPV5. (P_X^+/P_{Na}^+), were calculated from the recorded biionic reversal potentials for all five cations (MA^+, DMA^+, $TriMA^+$, $TetMA^+$ and $NMDG^+$) for both untreated and tTG-treated TRPV5 and subsequently plotted against the estimated diameter of each cation. For curve-fitting, the points from the graph plotting permeability ratios of the different organic cations (X) versus the estimated diameters, the excluded volume considering friction of the permeating ion Eq. $P_X^+/P_{Na}^+ = k(1 - a/d)2/a$ was used where a is the organic cation diameter, k a constant factor and d is the minimal pore diameter. *Black dots* with *continuous line* and *black squares* with *dashed lines* indicate untreated and tTG-treated TRPV5, respectively. **j** The pore diameter of TRPV5 is reduced by tTG. *Asterisk* indicates significant difference from control ($n = 7$; $P < 0.05$). **k** Tentative working model to demonstrate the effect of tTG on the pore size of TRPV5. The *upper panels* demonstrate the control situation and the *lower panels* depict the case upon tTG treatment. In the absence of tTG, Na^+ and Ca^{2+} can be transported through the pore. Na^+ flows continuously whereas, Ca^{2+} moves gradually from one Ca^{2+}-binding pocket to another in the pore of TRPV5. After tTG treatment, the continuous Na^+ transport is less inhibited whereas the gradual transport of Ca^{2+} is more severely blocked, as the pockets may not be accessible for Ca^{2+} ions

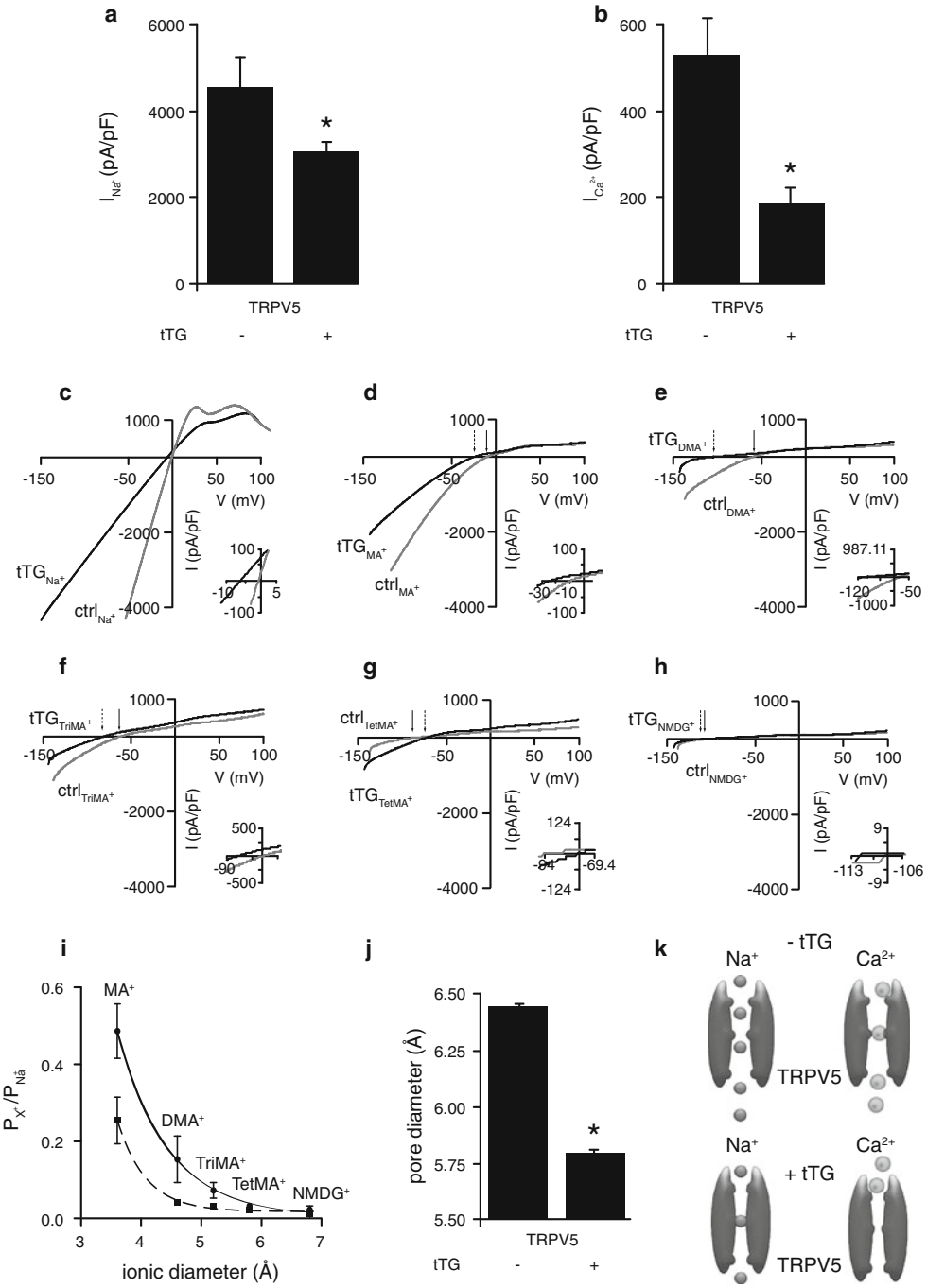

Taken together, our observations suggest that the apically secreted tTG functions as an inhibitor of TRPV5 and thereby contributes to the regulation of body Ca^{2+} homeostasis. Currently, it remains unclear whether an increased urinary tTG concentration is observed in conditions related to defective Ca^{2+} handling. One could envision several pathological conditions in which tTG reaches higher urinary concentrations, due to increased tissue damage or secretion of the enzyme. As such, rats with experimentally induced diabetes and diabetic nephropathy have increased renal tTG expression and activity resulting in abnormal extracellular crosslinking.

Here, we delineate a potential molecular mechanism by which tTG can inhibit TRPV5 channel activity by changing the pore diameter. This reduction is functionally coupled to crosslinking of the channel and seems to occur in a

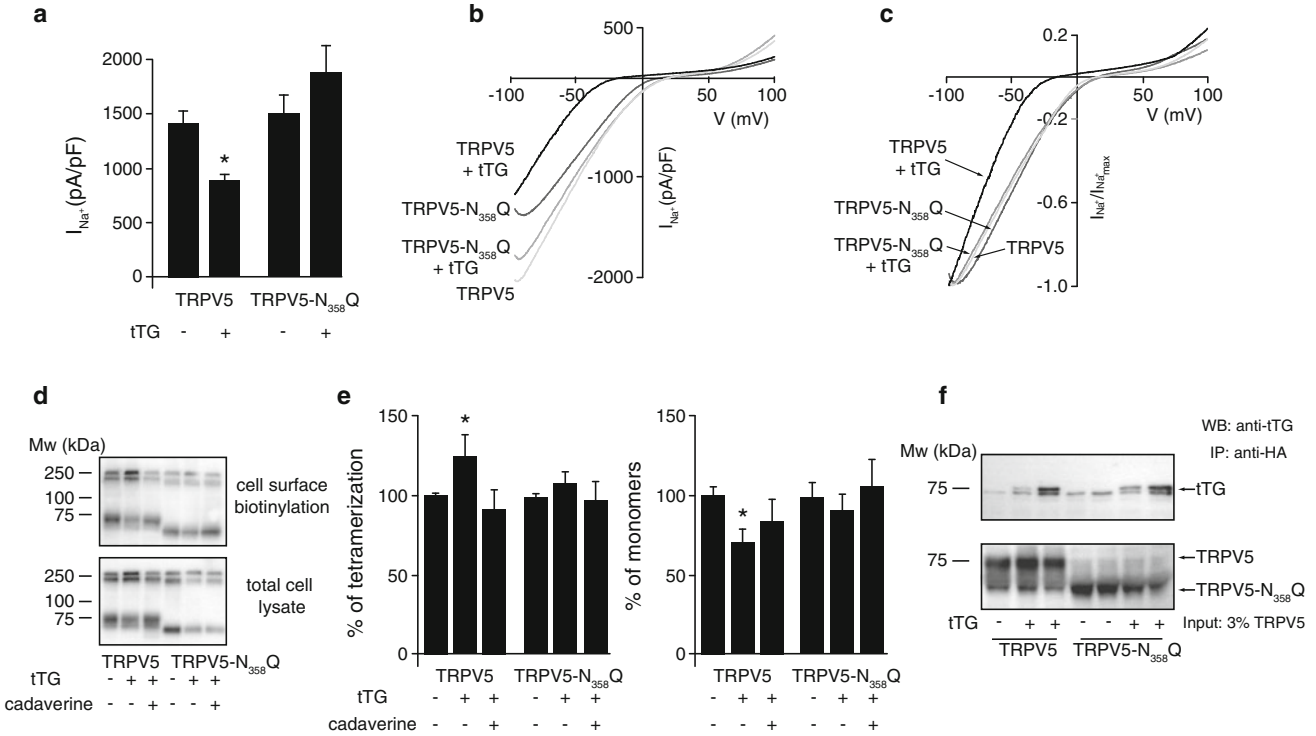

Fig. 4 N-glycosylation-deficient mutant TRPV5 is insensitive to tTG-mediated inhibition. **a** Na^+ currents were measured from wild-type TRPV5 and N-glycosylation-deficient TRPV5-N358Q mutant channels. The cells were subjected to 6-h tTG treatment (1 μg/ml) before the current measurement. Data are shown as mean ± SEM. *Asterisk* indicates significant difference from the cells expressing either wild-type or N-glycosylation-deficient mutant TRPV5 ($n = 11$; $P < 0.05$). **b** Representative Na^+ *I/V* relations of wild-type TRPV5 and TRPV5-N358Q in the absence or presence of purified transglutaminase. **c** Na^+ currents from **b** were normalized to I^+_{Na} max for better comparison and plotted as current voltage relationship. **d** Cell surface biotinylation of HEK293 cells transiently expressing HA-TRPV5 or HA-TRPV5-N358Q, after for 6 h of tTG treatment (1 μg/ml) tTG. The *upper* and *lower panels* represent the biotinylated cell surface fractions and the total cell lysates, respectively. **e** Semi-quantitative analysis of (**d**). The *left graph* shows the percentage of tTG-induced multimer formation of TRPV5, *right graph* illustrates the tTG-induced changes in the monomeric form of TRPV5. **f** Wild-type TRPV5 and TRPV5-N358Q bind tTG with equal efficiency. HA-tagged wild-type TRPV5 or TRPV5-N358Q was immunoprecipitated with HA-antibody from transiently transfected HEK293 cells. The precipitated fractions were incubated overnight at 4°C with 1 μg/ml purified tTG in EDTA-containing Ca^{2+}-free buffer to prevent any enzymatic activity of tTG and proteolysis. The beads with TRPV5 and tTG were successively washed and subjected to SDS–PAGE followed by anti-tTG antibody CUB 7402 (Abcam) or anti-TRPV5 immunoblot, respectively

N-glycosylation-dependent manner. Further studies are needed to establish the physiological role of tTG in regulating TRPV5-dependent Ca^{2+} transport.

Acknowledgments This work was financially supported by grants from the Dutch Kidney Foundation (C06.2170), the Netherlands Organization for Scientific Research (NWO-ALW 814.02.001, NWO-ALW 816.02.003, NWO-CW 700.55.302, ZonMw 9120.6110, A. ZonMw 9120.8026). J. Hoenderop is supported by a EURYI award. Part of our results was previously reported as an abstract at the annual meeting of the American Society of Nephrology October 27–November 1, 2009, San Diego, CA, USA.

Ethical standards All experimental work performed complies with the current laws of The Netherlands.

Conflict of interest The authors declare that they have no conflict of interest.

References

1. Aeschlimann D, Paulsson M (1991) Cross-linking of laminin-nidogen complexes by tissue transglutaminase. A novel mechanism for basement membrane stabilization. J Biol Chem 266:15308–15317
2. Barry PH (1994) JPCalc, a software package for calculating liquid junction potential corrections in patch-clamp, intracellular, epithelial and bilayer measurements and for correcting junction potential measurements. J Neurosci Methods 51:107–116
3. Beninati S, Senger DR, Cordella-Miele E, Mukherjee AB, Chackalaparampil I, Shanmugam V, Singh K, Mukherjee BB (1994) Osteopontin: its transglutaminase-catalyzed posttranslational modifications and cross-linking to fibronectin. J Biochem 115:675–682
4. Bindels RJ, Hartog A, Timmermans J, Van Os CH (1991) Active Ca^{2+} transport in primary cultures of rabbit kidney CCD: stimulation by 1,25-dihydroxyvitamin D_3 and PTH. Am J Physiol 261:F799–F807

5. Boros S, Kamps B, Wunderink L, de Bruijn W, de Jong WW, Boelens WC (2004) Transglutaminase catalyzes differential crosslinking of small heat shock proteins and amyloid-beta. FEBS Lett 576:57–62
6. Broome AM, Ryan D, Eckert RL (2003) S100 protein subcellular localization during epidermal differentiation and psoriasis. J Histochem Cytochem 51:675–685
7. Cha SK, Jabbar W, Xie J, Huang CL (2007) Regulation of TRPV5 single-channel activity by intracellular pH. J Membr Biol 220:79–85
8. Cha SK, Ortega B, Kurosu H, Rosenblatt KP, Kuro OM, Huang CL (2008) Removal of sialic acid involving Klotho causes cell-surface retention of TRPV5 channel via binding to galectin-1. Proc Natl Acad Sci USA 105:9805–9810
9. Chang Q, Hoefs S, van der Kemp AW, Topala CN, Bindels RJ, Hoenderop JG (2005) The beta-glucuronidase klotho hydrolyzes and activates the TRPV5 channel. Science 310:490–493
10. Cheng X, Jin J, Hu L, Shen D, Dong XP, Samie MA, Knoff J, Eisinger B, Liu ML, Huang SM, Caterina MJ, Dempsey P, Michael LE, Dlugosz AA, Andrews NC, Clapham DE, Xu H (2010) TRP channel regulates EGFR signaling in hair morphogenesis and skin barrier formation. Cell 141:331–343
11. D'Souza DR, Wei J, Shao Q, Hebert MD, Subramony SH, Vig PJ (2006) Tissue transglutaminase crosslinks ataxin-1: possible role in SCA1 pathogenesis. Neurosci Lett 409:5–9
12. El Nahas AM, Abo-Zenah H, Skill NJ, Bex S, Wild G, Griffin M, Johnson TS (2004) Elevated epsilon-(gamma-glutamyl)lysine in human diabetic nephropathy results from increased expression and cellular release of tissue transglutaminase. Nephron Clin Pract 97:c108–c117
13. Fesus L, Piacentini M (2002) Transglutaminase 2: an enigmatic enzyme with diverse functions. Trends Biochem Sci 27:534–539
14. Gambetti S, Dondi A, Cervellati C, Squerzanti M, Pansini FS, Bergamini CM (2005) Interaction with heparin protects tissue transglutaminase against inactivation by heating and by proteolysis. Biochimie 87:551–555
15. Hoenderop JG, Bindels RJ (2008) Calciotropic and magnesiotropic TRP channels. Physiology (Bethesda) 23:32–40
16. Hoenderop JG, Nilius B, Bindels RJ (2005) Calcium absorption across epithelia. Physiol Rev 85:373–422
17. Hoenderop JG, van der Kemp AW, Hartog A, van de Graaf SF, van Os CH, Willems PH, Bindels RJ (1999) Molecular identification of the apical Ca^{2+} channel in 1,25-dihydroxyvitamin D3-responsive epithelia. J Biol Chem 274:8375–8378
18. Hoenderop JG, van Leeuwen JP, van der Eerden BC, Kersten FF, van der Kemp AW, Merillat AM, Waarsing JH, Rossier BC, Vallon V, Hummler E, Bindels RJ (2003) Renal Ca^{2+} wasting, hyperabsorption, and reduced bone thickness in mice lacking TRPV5. J Clin Invest 112:1906–1914
19. Hoenderop JG, Voets T, Hoefs S, Weidema F, Prenen J, Nilius B, Bindels RJ (2003) Homo- and heterotetrameric architecture of the epithelial Ca^{2+} channels TRPV5 and TRPV6. EMBO J 22:776–785
20. Huang L, Haylor JL, Hau Z, Jones RA, Vickers ME, Wagner B, Griffin M, Saint RE, Coutts IG, El Nahas AM, Johnson TS (2009) Transglutaminase inhibition ameliorates experimental diabetic nephropathy. Kidney Int 76:383–394
21. Ikee R, Kobayashi S, Hemmi N, Saigusa T, Namikoshi T, Yamada M, Imakiire T, Kikuchi Y, Suzuki S, Miura S (2007) Involvement of transglutaminase-2 in pathological changes in renal disease. Nephron Clin Pract 105:c139–c146
22. Kaartinen MT, El-Maadawy S, Rasanen NH, McKee MD (2002) Tissue transglutaminase and its substrates in bone. J Bone Miner Res 17:2161–2173
23. Lee MY, Chung S, Bang HW, Baek KJ, Uhm D (1997) Modulation of large conductance Ca^{2+}-activated K^+ channel by Galphah (transglutaminase II) in the vascular smooth muscle cell. Pflugers Arch 433:671–673
24. Lehen'kyi V, Beck B, Polakowska R, Charveron M, Bordat P, Skryma R, Prevarskaya N (2007) TRPV6 is a Ca^{2+} entry channel essential for Ca^{2+}-induced differentiation of human keratinocytes. J Biol Chem 282:22582–22591
25. Liu SY, Huang HC, Li XM (2005) Tissue transglutaminase and renal fibrosis. Sheng Li Ke Xue Jin Zhan 36:314–318
26. Loffing J, Loffing-Cueni D, Valderrabano V, Klausli L, Hebert SC, Rossier BC, Hoenderop JG, Bindels RJ, Kaissling B (2001) Distribution of transcellular calcium and sodium transport pathways along mouse distal nephron. Am J Physiol Renal Physiol 281:F1021–F1027
27. Lorand L, Graham RM (2003) Transglutaminases: crosslinking enzymes with pleiotropic functions. Nat Rev Mol Cell Biol 4:140–156
28. Lu P, Boros S, Chang Q, Bindels RJ, Hoenderop JG (2008) The beta-glucuronidase klotho exclusively activates the epithelial Ca^{2+} channels TRPV5 and TRPV6. Nephrol Dial Transpl 23:3397–3402
29. Nilius B, Prenen J, Vennekens R, Hoenderop JG, Bindels RJ, Droogmans G (2001) Modulation of the epithelial calcium channel, ECaC, by intracellular Ca^{2+}. Cell Calcium 29:417–428
30. Okano T, Tsugawa N, Morishita A, Kato S (2004) Regulation of gene expression of epithelial calcium channels in intestine and kidney of mice by 1alpha, 25-dihydroxyvitamin D3. J Steroid Biochem Mol Biol 89–90:335–338
31. Pinkas DM, Strop P, Brunger AT, Khosla C (2007) Transglutaminase 2 undergoes a large conformational change upon activation. PLoS Biol 5:e327
32. Priglinger SG, May CA, Neubauer AS, Alge CS, Schonfeld CL, Kampik A, Welge-Lussen U (2003) Tissue transglutaminase as a modifying enzyme of the extracellular matrix in PVR membranes. Invest Ophthalmol Vis Sci 44:355–364
33. Raghunath M, Hopfner B, Aeschlimann D, Luthi U, Meuli M, Altermatt S, Gobet R, Bruckner-Tuderman L, Steinmann B (1996) Cross-linking of the dermo-epidermal junction of skin regenerating from keratinocyte autografts. Anchoring fibrils are a target for tissue transglutaminase. J Clin Invest 98:1174–1184
34. Ruse M, Lambert A, Robinson N, Ryan D, Shon KJ, Eckert RL (2001) S100A7, S100A10, and S100A11 are transglutaminase substrates. Biochemistry 40:3167–3173
35. Scarpellini A, Germack R, Lortat-Jacob H, Muramatsu T, Billett E, Johnson T, Verderio EA (2009) Heparan sulfate proteoglycans are receptors for the cell-surface trafficking and biological activity of transglutaminase-2. J Biol Chem 284:18411–18423
36. Shweke N, Boulos N, Jouanneau C, Vandermeersch S, Melino G, Dussaule JC, Chatziantoniou C, Ronco P, Boffa JJ (2008) Tissue transglutaminase contributes to interstitial renal fibrosis by favoring accumulation of fibrillar collagen through TGF-beta activation and cell infiltration. Am J Pathol 173:631–642
37. Skill NJ, Griffin M, El Nahas AM, Sanai T, Haylor JL, Fisher M, Jamie MF, Mould NN, Johnson TS (2001) Increases in renal epsilon-(gamma-glutamyl)-lysine crosslinks result from compartment-specific changes in tissue transglutaminase in early experimental diabetic nephropathy: pathologic implications. Lab Invest 81:705–716
38. Skill NJ, Johnson TS, Coutts IG, Saint RE, Fisher M, Huang L, El Nahas AM, Collighan RJ, Griffin M (2004) Inhibition of transglutaminase activity reduces extracellular matrix accumulation induced by high glucose levels in proximal tubular epithelial cells. J Biol Chem 279:47754–47762
39. Suzuki Y, Landowski CP, Hediger MA (2008) Mechanisms and regulation of epithelial Ca^{2+} absorption in health and disease. Annu Rev Physiol 70:257–271

40. van de Graaf SF, Bindels RJ, Hoenderop JG (2007) Physiology of epithelial Ca^{2+} and Mg^{2+} transport. Rev Physiol Biochem Pharmacol 158:77–160
41. van de Graaf SF, Boullart I, Hoenderop JG, Bindels RJ (2004) Regulation of the epithelial Ca^{2+} channels TRPV5 and TRPV6 by 1alpha, 25-dihydroxy vitamin D3 and dietary Ca^{2+}. J Steroid Biochem Mol Biol 89–90:303–308
42. van de Graaf SF, Hoenderop JG, Gkika D, Lamers D, Prenen J, Rescher U, Gerke V, Staub O, Nilius B, Bindels RJ (2003) Functional expression of the epithelial Ca^{2+} channels (TRPV5 and TRPV6) requires association of the S100A10-annexin 2 complex. EMBO J 22:1478–1487
43. Verderio EA, Telci D, Okoye A, Melino G, Griffin M (2003) A novel RGD-independent cel adhesion pathway mediated by fibronectin-bound tissue transglutaminase rescues cells from anoikis. J Biol Chem 278:42604–42614
44. Vig PJ, Wei J, Shao Q, Hebert MD, Subramony SH, Sutton LT (2007) Role of tissue transglutaminase type 2 in calbindin-D28k interaction with ataxin-1. Neurosci Lett 420:53–57